PNAS RESEARCH ARTICLE | CELL BIOLOGY

α-fluoro-β-alanine functions as a β-arrestin1-biased ligand of S1PR2 to upregulate DPD expression in cancer cells

Mingyong Tan[a], Hanbing Shao[a], Xinan Zhang[a], Yuyao Cheng[a], Zhimeng Sun[b], Ming Yang[b], Siyuan Mu[b], Weishi Liang[c,d], Bo Han[c,d], Xinfeng Wu[b], Xiaohui Liu[b], Yong Hai[c,d], Shuxiang Cui[a,c,1], and Xianjun Qu[b,c,1]

Edited by John J. G. Tesmer, Purdue University, West Lafayette, IN; received December 16, 2025; accepted June 18, 2026 by Editorial Board Member Melanie H. Cobb

α-fluoro-β-alanine (FBAL), a catabolite of the chemotherapeutic agent 5-fluorouracil (5-FU), has attracted significant attention due to its cardiotoxicity and neurotoxicity. However, its association with 5-FU resistance, a major obstacle in cancer treatment, has rarely been reported. In this study, FBAL was identified as a β-arrestin1-biased ligand of sphingosine 1-phosphate receptor 2 (S1PR2), which upregulates dihydropyrimidine dehydrogenase (DPD) expression and drives 5-FU resistance in colorectal cancer. Mechanistically, following exposure to FBAL, S1PR2, a G protein–coupled receptor (GPCR), is phosphorylated by recruiting G protein–coupled receptor kinase 6 (GRK6). Phosphorylated S1PR2 coupled with β-arrestin1, but not G proteins, to activate the MEK/ERK/AP-1 pathway and promote *DPYD* transcription. Ser343 was identified as the key phosphorylation site of S1PR2 using IP-MS analysis. This residue within the C-terminal domain mediates receptor interaction with β-arrestin-1 to activate the β-arrestin-1-dependent ERK pathway, as was confirmed in HCT116$^{S1PR2KO-\Delta C}$ cells and HCT116$^{S1PR2KO-S343A}$ cells. *In vivo*, mice bearing orthotopic xenografts of HCT116$^{S1PR2KO-S343A}$ cells exhibited significantly enhanced higher sensitivity to 5-FU treatment compared to those HCT116$^{S1PR2KO-WT}$ cells following FBAL. Taken together, this study showed that exposure to FBAL induces S1PR2 phosphorylation at Ser343 within the C-terminal mediated by GRK6, activating the β-arrestin1-dependent ERK pathway to upregulate DPD expression. This study not only delineates a phosphorylation-dependent signaling pathway in chemoresistance but also establishes S1PR2 as a promising therapeutic target for overcoming 5-FU resistance in cancer.

α-fluoro-β-alanine | sphingosine 1-phosphate receptor 2 | phosphorylation | G protein–coupled receptor kinase 6 | β-arrestin-1

Significance

Herein, we identify α-fluoro-β-alanine (FBAL), a metabolite of 5-fluorouracil (5-FU), as a β-arrestin1-biased ligand of sphingosine 1-phosphate receptor 2 (S1PR2) to upregulate dihydropyrimidine dehydrogenase (DPD) expression in cancer cells. DPD, the rate-limiting enzyme responsible for 5-FU catabolism, drives acquired resistance to 5-FU. Our study redefines FBAL from a toxic byproduct to a central driver of resistance and identifies S1PR2 as a promising target for restoring chemosensitivity in 5-FU-resistant cancers, thus offering a rationale for combining S1PR2 antagonists with fluoropyrimidine-based chemotherapy to overcome acquired resistance.

5-Fluorouracil (5-FU) remains a cornerstone of the chemotherapeutic management of various solid malignancies, including colorectal, breast, and gastric cancers (1). As a fluorinated pyrimidine analog, 5-FU exerts its cytotoxic effects primarily by inhibiting thymidylate synthase (TS) and its incorporation into RNA and DNA, disrupting essential nucleic acid metabolic processes, and leading to cell death (2). Despite its widespread use, resistance to 5-FU poses a significant challenge and often leads to therapeutic failure and disease recurrence. Resistance to 5-FU is multifactorial, with key mechanisms involving enhanced DNA repair, alterations in drug targets, and accelerated drug inactivation (3). The primary route of 5-FU catabolism is mediated by dihydropyrimidine dehydrogenase (DPD), the rate-limiting enzyme encoded by *DPYD* (4). DPD catalyzes the conversion of 5-FU to dihydrofluorouracil (DHFU), which is subsequently converted to α-fluoro-β-alanine (FBAL). Over 80% of the administered 5-FU is degraded through this metabolic pathway, underscoring the critical role of DPD in determining drug bioavailability and efficacy (5). Consequently, elevated DPD expression and activity are strongly correlated with acquired 5-FU resistance in multiple cancer types (6). Although much attention has been paid to the enzymatic function of DPD, the biological activities of its metabolic byproduct, FBAL, have been largely confined to its association with dose-limiting toxicities such as cardiotoxicity and neurotoxicity (7). FBAL is present at high levels in the blood and tumor tissues of patients receiving 5-FU and its derivatives at concentrations in the micromolar range (8), suggesting its potential for significant biological interactions. However, whether and how FBAL actively engages in signaling processes to influence treatment outcomes remain unclear.

Our group previously identified a link between sphingosine 1-phosphate receptor 2 (S1PR2) and the regulation of DPD expression in colorectal cancer cells (9). S1PR2, a member of the G protein–coupled receptor (GPCR) family, is typically activated by sphingosine-1-phosphate (S1P) and is involved in diverse physiological and pathological

Author affiliations: [a]Toxicology and Sanitary Chemistry, School of Public Health, Capital Medical University, Beijing 100069, China; [b]Pharmacology, School of Basic Medical Sciences, Capital Medical University, Beijing 100069, China; [c]Joint Laboratory for Research and Treatment of Spinal Cord Injury in Spinal Deformity, Capital Medical University, Beijing 100069, China; and [d]Department of Orthopedic Surgery, Beijing Chaoyang Hospital, Capital Medical University, Beijing 100020, China

Author contributions: M.T., S.C., and X.Q. designed research; M.T. performed research; H.S., X.Z., Y.C., Z.S., M.Y., S.M., W.L., B.H., X.W., X.L., and Y.H. contributed new reagents/analytic tools; M.T. analyzed data; and M.T., S.C., and X.Q. wrote the paper.

The authors declare no competing interest.

This article is a PNAS Direct Submission. J.J.G.T. is a guest editor invited by the Editorial Board.

[1]To whom correspondence may be addressed. Email: cuisx@ccmu.edu.cn or qxj@ccmu.edu.cn.

This article contains supporting information online at https://www.pnas.org/lookup/suppl/doi:10.1073/pnas.2533427123/-/DCSupplemental.

Published July 20, 2026.

processes, including inflammation, fibrosis, and cancer progression (10–12). We have demonstrated that the pharmacological inhibition of S1PR2 sensitizes cancer cells to 5-FU by downregulating DPD levels, suggesting a role in receptor-mediated chemoresistance (13). Unexpectedly, FBAL, which has previously been considered a biologically inert chemical, was found to play an essential role in the upregulation of DPD expression by activating S1PR2 (9). We hypothesized that FBAL functions as a ligand of S1PR2 to upregulate DPD expression in cancer cells. However, the underlying mechanisms have not been elucidated.

A pivotal mechanism for regulating GPCR activity and signaling specificity is the phosphorylation of the intracellular domains or C-terminals, which can dictate interactions with distinct downstream effector proteins. Different ligands can induce unique phosphorylation patterns in the same receptor, leading to divergent functional outcomes (14). Given that FBAL and the canonical S1PR2 ligand S1P produce different dynamics in DPD upregulation, we postulated that FBAL might induce a unique phosphorylation signature on S1PR2, thereby triggering a signaling cascade distinct from that of S1P and ultimately promoting *DPYD* transcription to confer 5-FU resistance.

In this study, we identified FBAL as a biased ligand of S1PR2. FBAL binds directly to S1PR2, leading to the phosphorylation of the S343 within the C-terminus tail of S1PR2 mediated by G protein–coupled receptor kinase 6 (GRK6). This FBAL-driven phosphorylation of S1PR2 facilitates the recruitment of β-arrestin1 and the subsequent sustained activation of the mitogen-activated protein kinase kinase (MEK)/extracellular signal-regulated kinase (ERK) pathway and AP-1 transcription factor complex, culminating in enhanced *DPYD* promoter activity and DPD expression. These findings reveal a previously unrecognized metabolic feedback loop, wherein a catabolite of 5-FU triggers a specific receptor phosphorylation event to drive 5-FU degradation, thereby sustaining chemoresistance. These insights not only deepen our understanding of 5-FU resistance mechanisms but also highlight the FBAL-induced S1PR2 phosphorylation axis as a promising therapeutic target for overcoming 5-FU resistance.

Results

FBAL Attenuated the Anticancer Activity of 5-FU by Upregulating DPD Expression. To measure the effect of FBAL on 5-FU activity, cancer cells were exposed to FBAL and the inhibition rates between cells treated with 5-FU alone and those cotreated with 5-FU and FBAL were compared. 5-FU (10 μM) strongly inhibited the growth of HCT116 and SW620 cells in vitro, whereas this antiproliferative effect of 5-FU was significantly attenuated in the presence of 50 μM FBAL (Fig. 1*A*). The impact of FBAL on 5-FU activity was further assessed by measuring changes in IC_{50} and Emax values. The IC_{50} values of 5-FU in HCT116 cells strongly increased from 10.58 μM in the absence of FBAL to 89.46 μM on exposure to FBAL (Fig. 1*B*) and from 45.05 μM in the absence of

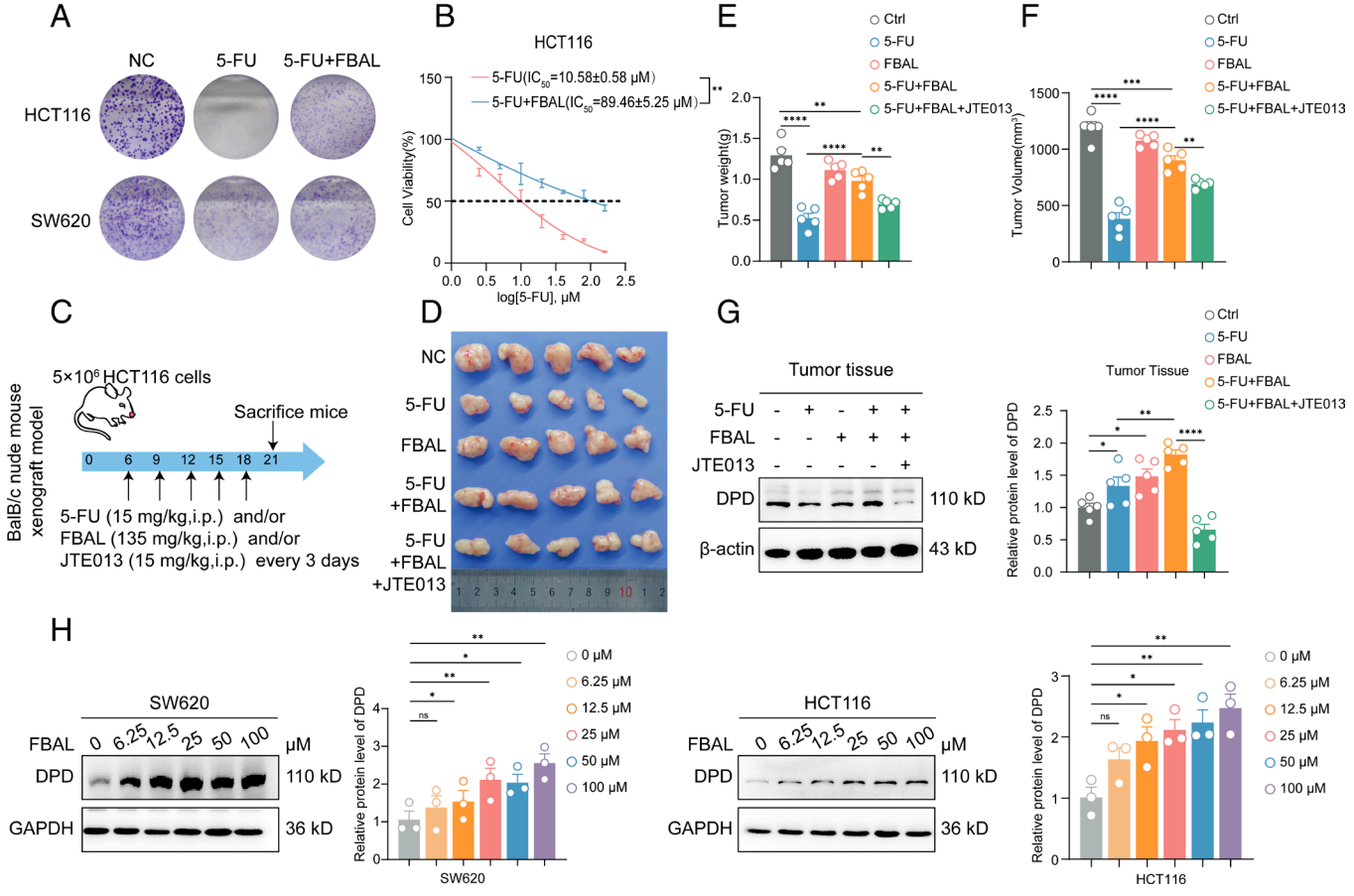

Fig. 1. FBAL attenuated the anticancer activity of 5-FU by upregulating DPD expression. (*A*) Exposed to 50 μM FBAL, the effect of 10 μM 5-FU on colony growth was attenuated in HCT116 (*Above*) and SW620 cells (*Bottom*). (*B*) The IC50s of 5-FU were significantly increased in the presence of 50 μM FBAL in HCT116 cells. (*C*) Schematic diagram of HCTT116 cells xenografted in nude mice (n = 5). (*D*) The images of HCT116 xenografts in different groups on day 21. (*E*) Tumor weights in different groups. (*F*) The average tumor volumes in different groups. (*G*) Western blotting analysis of DPD and β-actin in HCT116 xenografts. (*H*) Western blotting analysis of DPD and GAPDH in SW620 cells and HCT116 cells treated with FBAL in indicated concentrations. Data are mean ± SEM. **P* < 0.05, ***P* < 0.01, ****P* < 0.001, *****P* < 0.0001; ns: not significant. n = 3.

FBAL to 81.98 μM exposed to FBAL in SW620 cells (*SI Appendix,* Fig. S1*A*). The Emax values of 5-FU in HCT116 cells strongly reduced from 90.85% in the absence of FBAL to 55.47% exposed to FBAL (Fig. 1*B*) and from 74.32% in the absence of FBAL to 61.91% on exposure to FBAL in SW620 cells (*SI Appendix,* Fig. S1*A*). In vivo results confirmed the effect of FBAL on 5-FU activity. HCT116 cells were subcutaneously xenografted into nude mice (Fig. 1 *C* and *D*) and treated with 5-FU (15 mg/kg), FBAL (135 mg/kg), or JTE013 (15 mg/kg). Treatment with 5-FU alone inhibited HCT116 xenograft growth by 61% (Fig. 1 *E* and *F*). The body weight of the mice was not significantly affected by this dose of 5-FU (*SI Appendix,* Fig. S1*B*). FBAL alone (135 mg/kg) did not directly affect HCT116 xenograft growth (Fig. 1 *E* and *F*) but significantly attenuated 5-FU activity, showing that the inhibition rate of 5-FU was strongly reduced in the presence of FBAL (Fig. 1 *E* and *F*). Interestingly, JTE-013, a selective S1PR2 inhibitor (15), blocked the FBAL-induced attenuation of 5-FU activity (Fig. 1 *E* and *F*). The findings suggest that the effect of FBAL on the activity of 5-FU is associated with its ability to upregulate S1PR2 expression or activity in cancer cells.

Overexpression of DPD has frequently been identified as a major determinant of 5-FU resistance. We analyzed DPD levels in HCT116 xenografts to elucidate the mechanism of 5-FU resistance. HCT116 xenografts treated with 5-FU and FBAL exhibited higher levels of DPD expression than those treated with 5-FU alone, whereas higher DPD levels were not achieved in JTE-013-treated HCT116 xenografts (Fig. 1*G* and *SI Appendix,* Fig. S1 *C* and *D*). The FBAL-induced increase in DPD expression was also observed at the transcriptional level (*SI Appendix,* Fig. S1*E*). These results indicate that the upregulation of *DPYD* mRNA is associated with the diminished efficacy of 5-FU in the presence of FBAL. Supportive of this suggestion, in the presence of FBAL, DPD levels were significantly increased in HCT116 and SW620 cells in a concentration-dependent manner (Fig. 1*H*). RT-qPCR analysis showed a concentration-dependent increase in mRNA levels of *DPYD* in HCT116 and SW620 cells (*SI Appendix,* Fig. S1*F*). TS, an enzymatic target of 5-FU, has been implicated in the development of 5-FU resistance (16). The levels were analyzed in the presence of FBAL. No significant change in TS expression was observed in the presence of FBAL at either the protein or mRNA level in HCT116 xenografts (*SI Appendix,* Fig. S2 *A–D*) or in cultured HCT116 and SW620 cells (*SI Appendix,* Fig. S2 *E* and *F*). Thus, FBAL attenuated the antitumor activity of 5-FU by upregulating DPD expression, but not that of TS.

FBAL Upregulated DPD Expression Through Activating S1PR2 in Colonic Cancer. Although we reported a link between S1PR2 activation and DPD expression in 2020 (17), the mechanisms underlying S1PR2 activation remain unclear. This association has been observed across a large panel of cancer cell lines (*SI Appendix,* Fig. S3*A*). Supporting this link, S1PR2 silencing downregulated DPD expression at both the mRNA level (*SI Appendix,* Fig. S3*B*), and protein levels (*SI Appendix,* Fig. S3*C*) in the HCT116 and SW620 cells, respectively. In the presence of FBAL, DPD levels were significantly upregulated in siNC-transfected SW620 and HCT116 cells, whereas no such upregulation was observed in *S1PR2*-silenced cells (Fig. 2*A* and *SI Appendix,* Fig. S3*D*). The FBAL-induced upregulation through activating S1PR2 activation was blocked by exposure to JTE-013 in HCT116 and SW620 cells (Fig. 2*B* and *SI Appendix,* Fig. S3*E*). To identify FBAL, which is derived from the metabolism of 5-FU catalyzed by DPD, we performed experiments using 5-FU and gimeracil (CDHP), an inhibitor of DPD (18). The results showed that DPD expression was upregulated by 5-FU treatment in HCT116 and SW620 cells (*SI Appendix,* Fig. S3*F*). However, when these cells were exposed to 5-FU and CDHP, the 5-FU-induced upregulation of DPD was significantly abolished. These results suggest that the upregulation of DPD following 5-FU treatment requires DPD enzymatic activity, supporting the idea that FBAL is derived from the DPD-catalyzed metabolism of 5-FU (*SI Appendix,* Fig. S3*F*). Together with our previous findings, these results indicated that FBAL upregulates DPD expression by activating S1PR2 expression. The attenuation of 5-FU activity by FBAL could be reversed by suppressing S1PR2 using JTE-013 (Fig. 2*C*). Consistently, the IC_{50} values of 5-FU were strongly increased from 14.74 ± 1.948 μM in the absence of FBAL to 82.89 ± 2.490 μM in the presence of FBAL in $HCT116^{shNC}$ cells, whereas the IC_{50} values of 5-FU were not increased in $HCT116^{shS1PR2}$ whether or not exposed to FBAL (Fig. 2*D*). These data suggest that S1PR2 silencing blocked the FBAL-induced increase in the IC_{50} values of 5-FU.

The effect of FBAL on 5-FU activity by activating S1PR2 was confirmed in nude mice orthotopically implanted with $HCT116^{shNC}$ and $HCT116^{shS1PR2}$ cells labeled with Luc and GFP. $HCT116^{shNC}$ and $HCT116^{shS1PR2}$ xenografts were exposed to the same scheme (Fig. 2*E*): 5-FU (15 mg/kg i.p.) or 5-FU+FBAL (135 mg/kg i.p.) every 3 d for a continuous 21 d. 5-FU at this dose did not significantly affect the body weight of mice (*SI Appendix,* Fig. S3*G*). 5-FU strongly inhibited the growth of $HCT116^{shNC}$ xenografts; however, this effect of 5-FU was attenuated in the presence of FBAL (Fig. 2 *F* and *G*). Comparably, S1PR2 silencing slowed the growth of $HCT116^{shS1PR2}$ xenografts, and treatment with 5-FU further inhibited the growth of $HCT116^{shS1PR2}$ xenografts. Compared with the impact of FBAL on 5-FU activity in the $HCT116^{shNC}$ xenograft, FBAL did not significantly impact on 5-FU activity in $HCT116^{shS1PR2}$ xenograft (Fig. 2 *F* and *G*). Taken together, these results suggest that FBAL attenuated the anticancer activity of 5-FU by activating S1PR2. As an endogenous ligand, S1P activates S1PR2 to regulate various physiological functions (19). Differences between S1P and FBAL in the upregulation of DPD expression were compared between cancer cells. As expected, FBAL-induced upregulation of DPD expression, which was prolonged and persisted for up to 60 min (Fig. 2*H* and *SI Appendix,* Fig. S3 *H* and *I*). Comparatively, S1P activation of S1PR2 to upregulate DPD expression was transient, occurring only within 5 min (Fig. 2*H* and *SI Appendix,* Fig. S3 *H* and *I*). Thus, the upregulation of DPD by FBAL through the activation of S1PR2 exhibited a distinct pattern than that of its natural ligand S1P, which transiently activated S1PR2. Collectively, FBAL attenuated 5-FU activity by upregulating DPD and sustaining S1PR2 activation.

FBAL Activated the ERK Signaling Pathway Independently of S1P. Activation of the ERK signaling pathway by S1PR2 is well established. FBAL significantly induced ERK phosphorylation in HCT116 xenografts, which was significantly reduced by exposure to 15 mg/kg JTE-013 (Fig. 3*A* and *SI Appendix,* Fig. S4*A*). It is well established that ERK activation by GPCRs is mediated via two canonical pathways: a G protein–dependent pathway and a β-arrestin-dependent pathway (20). As a classic GPCR, S1PR2 can follow two distinct pathways. As an endogenous ligand, S1P activates the ERK pathway via S1PR2 (21–23). To exclude the role of S1P in FBAL activation of the ERK pathway in HCT116 xenografts, we analyzed S1P levels in the tumor tissues and serum of mice. No significant differences in S1P levels were observed between FBAL- and NS-treated HCT116 xenografts or in the serum of the different groups of mice (*SI Appendix,* Fig. S4 *B* and *C*). These results indicate that FBAL activated the ERK pathway by directly activating S1PR2, but not by elevating S1P levels to activate S1PR2.

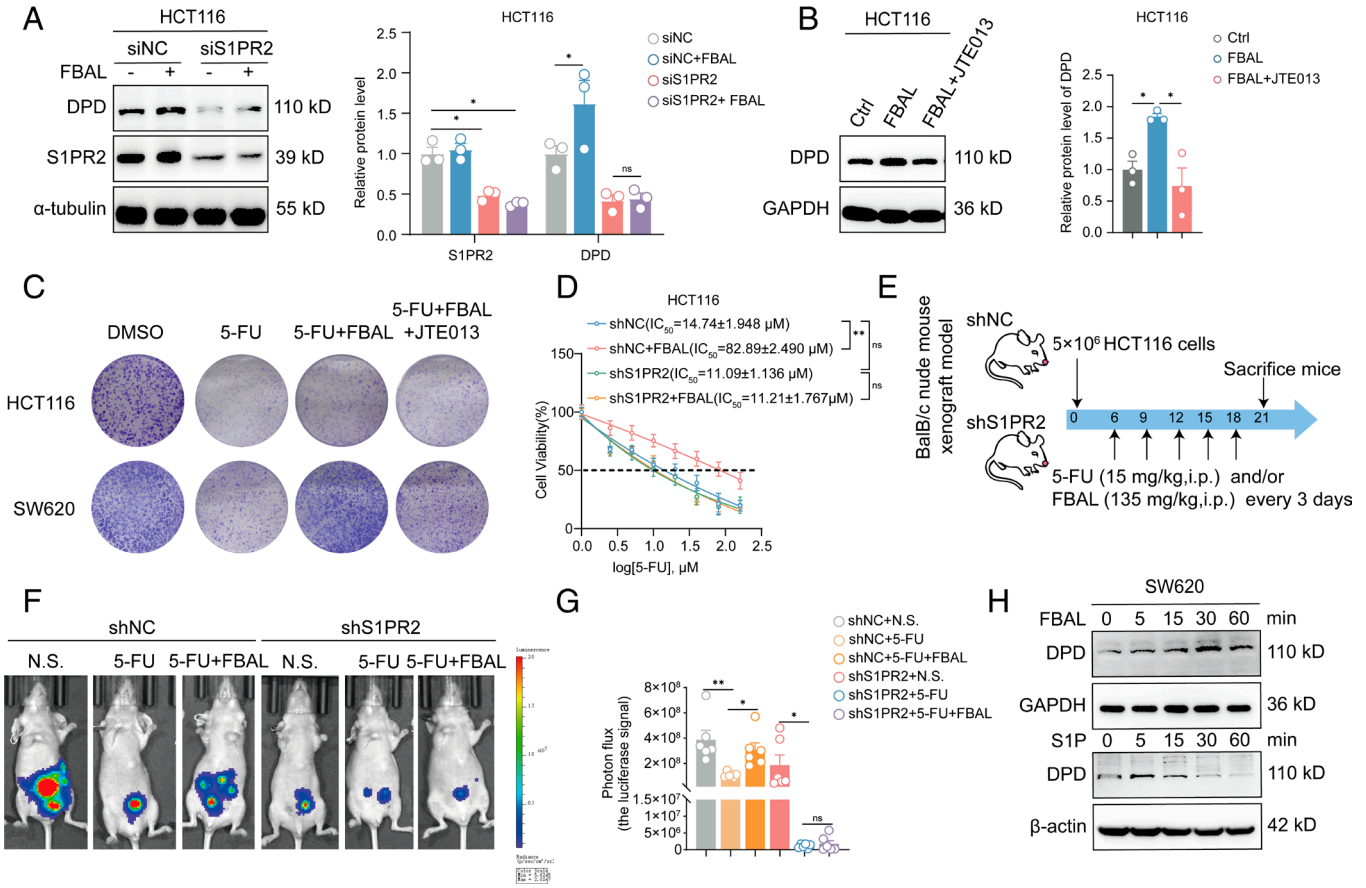

Fig. 2. FBAL upregulated DPD expression through activating S1PR2 in colonic cancer. (*A*) Silencing of S1PR2 blocked FBAL-induced DPD expression in HCT116 cells. (*B*) 50 μM FBAL induced DPD expression and 20 μM JTE-013 blocked FBAL-induced DPD expression in HCT116 cells. (*C*) 50 μM FBAL attenuated 5-FU activity in the inhibition of cancer colony formation. JTE-013 blocked the FBAL-induced attenuation of the 5-FU activity in HCT116 cells (*Above*) and SW620 cells (*Bottom*). (*D*) Comparison of IC_{50} values of 5-FU in $HCT116^{shNC}$ cells and $HCT116^{shS1PR2}$ cells with or without FBAL. (*E*) Schematic diagram of the experiment protocol using HCT116-labeled Luc and GFP cells orthotopically xenografted in nude mice (n = 6). (*F*) The growth of HCT116 xenografts as monitored under in vivo imaging system (IVIS). (*G*) Statistical analysis of total flux from IVIS bioluminescence images. (*H*) Western blotting analysis of DPD, GAPDH and β-actin expression in SW620 cells treated with 10 μM FBAL or 10 μM S1P as the indicated times. Data are mean ± SEM. **P* < 0.05, ***P* < 0.01, ****P* < 0.001, *****P* < 0.0001; ns: not significant, n = 3.

The FBAL-induced pattern of ERK activation was compared to that of the endogenous ligand S1P. Following 10 μM S1P binding, p-ERK levels rapidly and sharply increased at 5 min, followed by a rapid decline within 15 min in HCT116 and SW620 cells (Fig. 3*B* and *SI Appendix,* Fig. S4*D*). This pattern of ERK activation has been previously associated with the G protein–dependent signaling in certain contexts (24). Comparably, following 50 μM FBAL binding, the increase in the p-ERK levels was gradual and sustained (i.e., >60 min) and peaked at 60 min in HCT116 and SW620 cells (Fig. 3*C* and *SI Appendix,* Fig. S4*E*). This pattern has been reported to be consistent with the β-arrestin-dependent pathway (24).

The role of FBAL in mediating phosphorylation of ERK via S1PR2 was further evidenced by silencing of S1PR2, which inhibited the 50 μM FBAL-induced phosphorylation of ERK in $HCT116^{siS1PR2}$ cells and $SW620^{siS1PR2}$ cells (Fig. 3*D* and *SI Appendix,* Fig. S4*F*). Treatment with 20 μM JTE013 prevented the 50 μM FBAL-induced phosphorylation of ERK in HCT116 and SW620 cells (*SI Appendix,* Fig. S4 *G* and *H*). Conversely, overexpression of S1PR2 through *S1PR2* transfection followed by treatment with FBAL showed a time- (Fig. 3*E*) and dose-dependent (*SI Appendix,* Fig. S4*I*) increase in p-ERK in $HEK293T^{OE\text{-}S1PR2}$ cells but not in $HEK293T^{OE\text{-}NC}$ cells. Furthermore, S1PR2 purified from bacteria could directly bind FBAL (Fig. 3*F*). The dissociation constant (K_d) for FBAL-S1PR2 was about 0.3931 μM. Collectively, these results indicate that FBAL can activate the ERK signaling pathway and that the activation pattern is quite distinct from that of S1P.

Following FBAL Binding, S1PR2 Was Phosphorylated by Recruiting GRK6. Phosphorylation is a major regulator of GPCR signaling dynamics (25, 26). A significant increase in the phosphorylation of endogenous S1PR2 was observed upon exposure to 50 μM FBAL, as assessed by immunoprecipitation (IP) using an anti-phospho-serine/threonine antibody in HCT116 cells (Fig. 4*A*) and SW620 cells (*SI Appendix,* Fig. S5*A*). Exogenous S1PR2 was also phosphorylated following treatment with 50 μM FBAL in HEK293T cells transfected with *Flag-S1PR2* (Fig. 4*B*). These results indicate that S1PR2 is a phosphorylated protein that can be triggered by FBAL.

GPCR phosphorylation is performed by distinct GRKs to activate different downstream signaling cascades (27, 28). This raised the question of which GRK phosphorylates S1PR2. Owing to their tissue specificity and structural homology (29), we analyzed the levels of GRK6 and GRK2 in FBAL-treated cancer cells. The levels of GRK6, but not GRK2, significantly increased in a time-dependent manner within 60 min in SW620 (Fig. 4*C*) and HCT116 cells (*SI Appendix,* Fig. S5*B*) after FBAL treatment. Co-IP analysis revealed the binding of GRK6, but not GRK2, to S1PR2 in HCT116 (Fig. 4 *D* and *E*) and SW620 cells (*SI Appendix,* Fig. S5 *C* and *D*) after FBAL treatment.

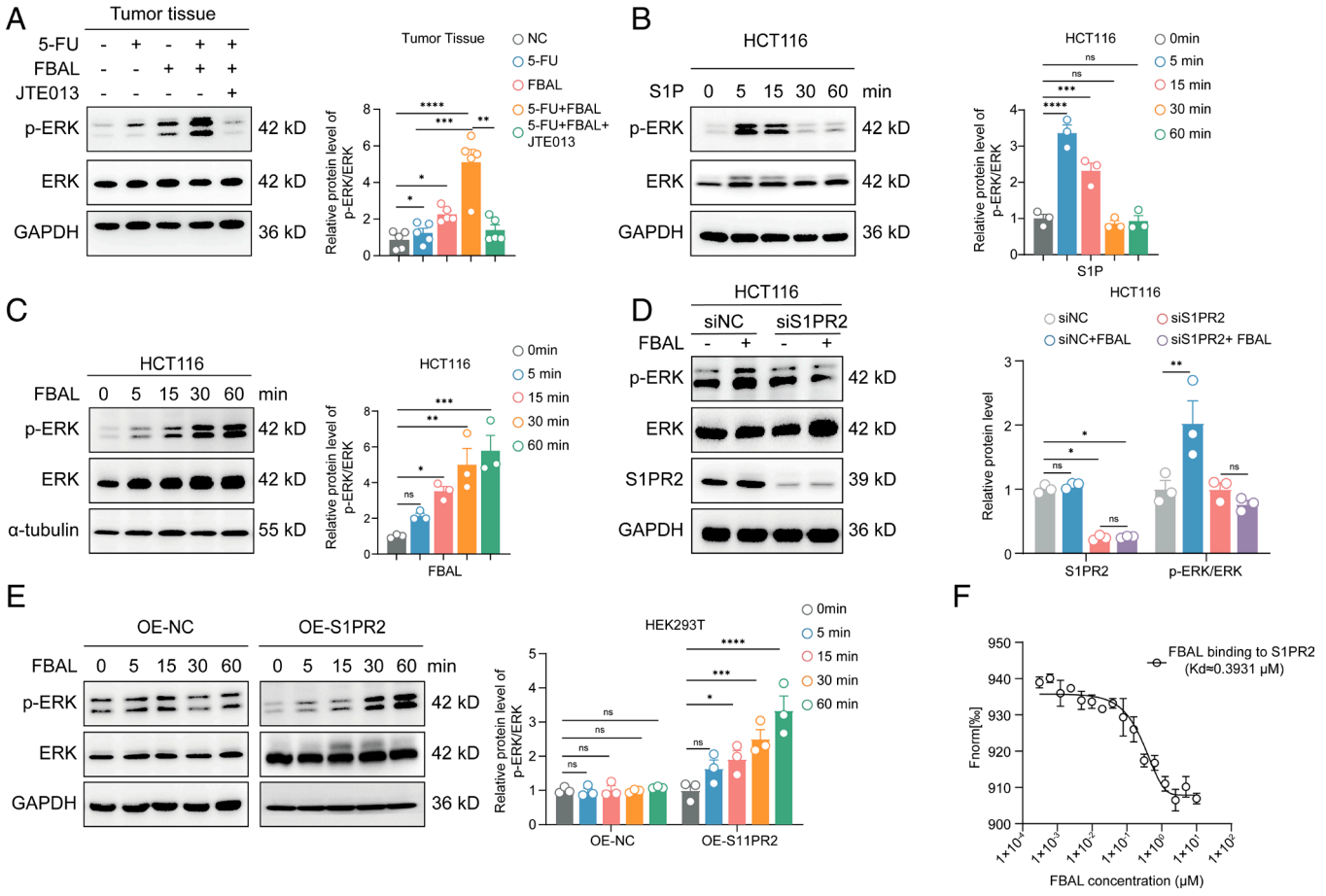

Fig. 3. FBAL activated the ERK signaling pathway independently of S1P. (*A*) Western blotting analysis of p-ERK, ERK, and GAPDH levels in HCT116 xenografts. (*B*) Western blotting analysis of p-ERK, ERK, and GAPDH levels in HCT116 cells following exposure to S1P at the indicated times. (*C*) Western blotting analysis of p-ERK, ERK, and α-tubulin in HCT116 cells exposed to FBAL at the indicated times. (*D*) Silencing of S1PR2 abrogated the 50 μM FBAL-induced increase of p-ERK in HCT116 cells. (*E*) HEK293T$^{OE\text{-}S1PR2}$ cells but not HEK293T$^{OE\text{-}NC}$ cells exhibited higher levels of p-ERK in a time-dependent manner following FBAL stimulation. (*F*) MST binding affinity between FBAL and S1PR2. Fnorm (%) represents the normalized fluorescence signal (Fnorm = F_hot/F_cold × 100%), where F_hot is the average fluorescence intensity during the steady-state thermophoresis phase (MST on) and F_cold is the initial fluorescence before the laser is turned on. Data are mean ± SEM. *P < 0.05, **P < 0.01, ***P < 0.001, ****P < 0.0001; ns: not significant, n = 3.

To identify the S1PR2 phosphorylation by GRK6, but not GRK2, cancer cells were exposed to GRK6-IN-1 (a GRK6 inhibitor) (30) and CCG258208 (a GRK2-IN-1) hydrochloride (a GRK2 inhibitor) (31), and then subjected to Co-IP assays. Following FBAL, GRK6-IN-1 (50 μM) but not CCG258208 hydrochloride (10 μM) effectively blocked S1PR2 phosphorylation in HCT116 (Fig. 4*F*) and SW620 cells (*SI Appendix,* Fig. S5*E*). GRK6 silencing also blocked FBAL-induced S1PR2 phosphorylation in HCT116 (Fig. 4*G*) and SW620 (*SI Appendix,* Fig. S5*F*). In the downstream signaling pathway, S1PR2 phosphorylation leads to ERK activation. As expected, silencing or inhibition of GRK6 blocked FBAL-induced phosphorylation of ERK (Fig. 4 *H* and *I* and *SI Appendix,* Fig. S5 *G* and *J*). However, GRK2 silencing did not prevent FBAL-induced ERK phosphorylation (*SI Appendix,* Fig. S5 *H* and *I*). Inhibition of GRK2 by CCG258208 hydrochloride failed to prevent the FBAL-induced phosphorylation of ERK (Fig. 4*I* and *SI Appendix,* Fig. S5*J*). Collectively, following FBAL binding, S1PR2 was phosphorylated by recruitment of GRK6.

FBAL Induced ERK Phosphorylation Through the β-Arrestin1-Dependent Pathway. β-arrestins are the essential regulators of GPCR signaling (32, 33). To identify which β-arrestin subtype acted as a signal transducer to mediate S1PR2 signaling, β-arrestin1 and β-arrestin2 were separately silenced, and p-ERK expression was then analyzed. The level of p-ERK was not changed in HCT116$^{siβ\text{-}arrestin1}$ and SW620$^{siβ\text{-}arrestin1}$ cells (Fig. 5*A* and *SI Appendix,* Fig. S6*A*) with or without 50 μM FBAL, whereas 50 μM FBAL significantly promoted ERK phosphorylation in HCT116$^{siβ\text{-}arrestin2}$ and SW620$^{siβ\text{-}arrestin2}$ cells (Fig. 5*B* and *SI Appendix,* Fig. S6*B*). Given that S1P is a balanced ligand of S1PR2 and is known to activate the ERK pathway, we sought to identify whether β-arrestin plays an essential role in S1P-mediated ERK activation. To this end, we individually knocked down β-arrestin1 and β-arrestin2 expression in HCT116 and SW620 cells. The results showed that S1P-induced ERK activation was not affected by the loss of either β-arrestin1 or β-arrestin2 alone (Fig. 5 *C* and *D* and *SI Appendix,* Fig. S6 *C* and *D*). Moreover, even when both β-arrestin1 and β-arrestin2 were simultaneously depleted, S1P still robustly activated the ERK pathway (*SI Appendix,* Fig. S6 *E* and *F*). These results indicate that FBAL activates the ERK signaling pathway in a β-arrestin1-dependent manner, whereas S1P mediates ERK activation β-arrestin-independently. Further the Co-IP assay identified the binding of S1PR2 with β-arrestin1 following 50 μM FBAL in HCT116 (Fig. 5*E*) and SW620 cells (*SI Appendix,* Fig. S6*G*). Co-IP analysis revealed S1PR2 binding to β-arrestin1 following 50 μM FBAL in HEK293T cells which were cotransfected with Flag-S1PR2 and mCherry-β-arrestin1 (Fig. 5*F*). It has been reported that balanced ligands induce receptor desensitization by recruiting β-arrestin following GPCR

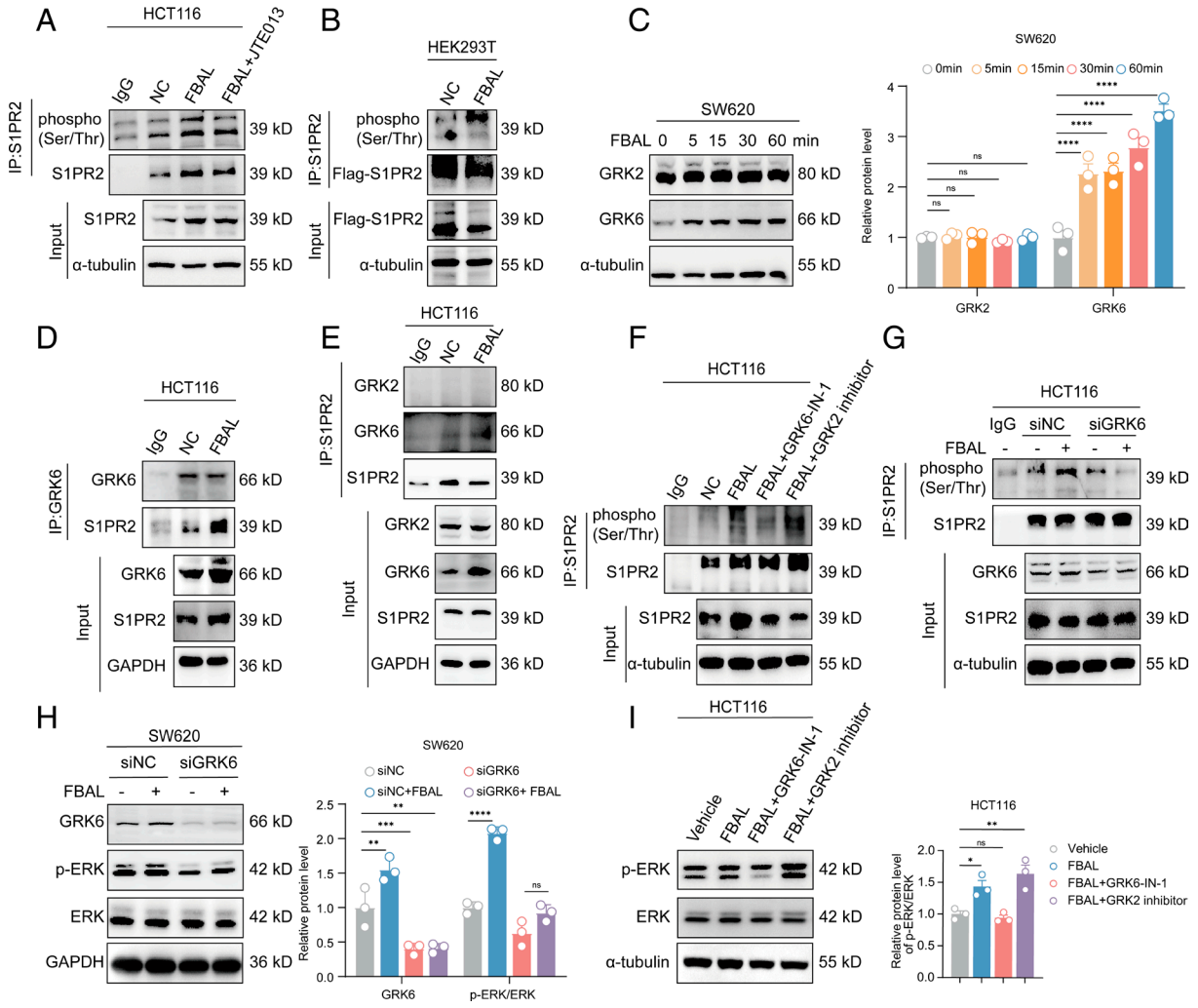

Fig. 4. Following FBAL binding, S1PR2 was phosphorylated by recruiting GRK6. (*A*) HCT116 cells were treated with 50 μM FBAL, and immunoblotting analysis was performed. p-S/T, serine/threonine phosphorylation. (*B*) HEK293T cells stably expressing Flag-S1PR2 were treated with 50 μM FBAL and immunoblotting analysis was performed. p-S/T, serine/threonine phosphorylation. (*C*) Western blotting of GRK6 and GRK2 in the FBAL-treated SW620 cells (50 μM). (*D*) Coimmunoprecipitation (Co-IP) analysis identified the binding of GRK6 with S1PR2 in HCT116 cells following treatment with 50 μM FBAL. (*E*) Co-IP analysis identified GRK6 but not GRK2 binding to S1PR2 in HCT116 cells following treatment with 50 μM FBAL. (*F*) Co-IP assay showed that the FBAL-induced phosphorylation of S1PR2 was blocked by 50 μM GRK6-IN-1 but not by 10 μM CCG258208 hydrochloride in HCT116 cells. (*G*) Silencing of GRK6 expression blocked S1PR2 phosphorylation in HCT116 cells. (*H*) Silencing of GRK6 failed to induce p-ERK upregulation by FBAL in SW620 cells. (*I*) Western blotting analysis of p-ERK and ERK levels following FBAL stimulation. 50 μM GRK6-IN-1 but not 10 μM CCG258208 hydrochloride blocked the FBAL-induced phosphorylation of ERK in HCT116 cells. Data are presented as mean ± SEM. **P* < 0.05, ***P* < 0.01, ****P* < 0.001, *****P* < 0.0001; ns: not significant, n = 3.

activation. To identify which β-arrestin isoform was recruited by S1P, HEK293T cells were cotransfected *S1PR2* with either β-arrestin1 or β-arrestin2. The Co-IP analysis showed that S1P promoted the binding of S1PR2 with β-arrestin2 but not with β-arrestin1 (*SI Appendix,* Fig. S6 *H* and *I*). These results suggest that FBAL and S1P engage distinct β-arrestin isoforms to mediate S1PR2 signaling, which FBAL selectively recruited β-arrestin1 and S1P specifically recruited β-arrestin2.

Activated S1PR2 can couple to Gαq, Gαi, and Gα12/13, which in turn catalyze the generation or release of second messenger molecules, such as Ca^{2+} and cAMP (34, 35). In this study, in response to S1P binding (10 μM), the Ca^{2+} levels were rapidly released at ~30 to 40 s and then steeply peaked at 5 s followed by a rapid decline within 200 s in HCT116 cells (Fig. 5*G*) and SW620 cells (*SI Appendix,* Fig. S7*A*), indicating that S1PR2 was activated by S1P coupled with the Gαq protein. Comparably, the levels of Ca^{2+} did not significantly change in the same cell lines following exposure to FBAL (50 μM) binding, suggesting that activated S1PR2 by FBAL was not coupled with the Gαq protein (Fig. 5*G* and *SI Appendix,* Fig. S7*A*). As expected, cAMP levels were dramatically reduced following S1P (10 μM) binding but not following 50 μM FBAL binding in HCT116 and SW620 cells (Fig. 5*H* and *SI Appendix,* Fig. S7*B*). Furthermore, pharmacological inhibition of the G protein by 100 ng/mL PTX, a Gαi-protein inhibitor (36), failed to block FBAL-induced ERK phosphorylation in HCT116 cells (Fig. 5*I*) and SW620 cells (*SI Appendix,* Fig. S7*C*). To demonstrate that S1P activated the ERK signaling pathway via Gαi, the cancer cells were exposed to S1P in the presence or absence of PTX. S1P alone significantly induced ERK phosphorylation in HCT116 (Fig. 5*J*) and SW620 cells (*SI Appendix,* Fig. S7*D*). However, when these cells were cotreated with S1P and PTX, the S1P-induced ERK phosphorylation was abolished (Fig. 5*J* and *SI Appendix,* Fig. S7*D*). These results indicated that S1P activates the ERK signaling pathway through a Gαi-dependent manner (Fig. 5*J* and *SI Appendix,* Fig. S7*D*). We further performed an active Rho pull-down assay to determine whether FBAL activated S1PR2 without engaging the Gα12/13 pathway. The result showed that FBAL failed to activate Gα12/13 (Fig. 5*K* and *SI Appendix,* Fig. S7*E*). In contrast, S1P robustly activated this protein. Collectively, these findings

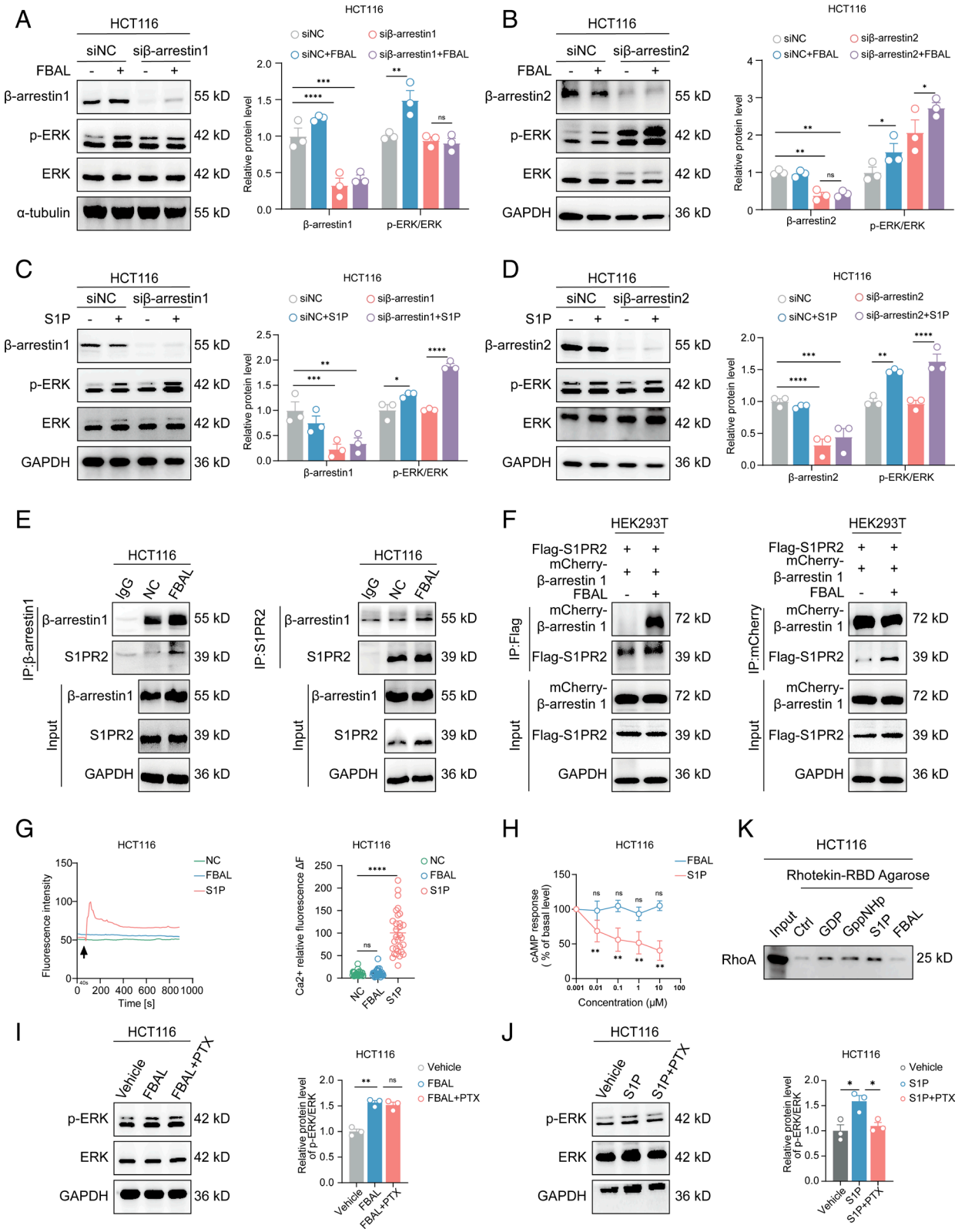

Fig. 5. FBAL induced ERK phosphorylation through the β-arrestin1-dependent pathway. (*A*) The levels of p-ERK did not change in HCT116$^{siβ\text{-}arrestin1}$ cells with or without 50 μM FBAL. (*B*) The levels of p-ERK were increased following 50 μM FBAL in HCT116$^{siβ\text{-}arrestin2}$ cells. (*C*) Levels of p-ERK did not change in HCT116$^{siβ\text{-}arrestin1}$ cells with or without 10 μM S1P. (*D*) Levels of p-ERK were significantly increased following 10 μM S1P in HCT116$^{siβ\text{-}arrestin2}$ cells. (*E*) Co-IP assay identified the binding of S1PR2 with β-arrestin1 following exposure to 50 μM FBAL in HCT116 cells. (*F*) Co-IP assay identified the binding of β-arrestin1 with S1PR2 following exposure to 50 μM FBAL in HEK293T cells cotransfected with the Flag-S1PR2 and the mCherry-β-arrestin1. (*G*) Fluo-4-AM probe analysis showed a sharp increase of Ca^{2+} in the cytoplasm within 40 s and a dramatic decrease of Ca^{2+} within 100 s in response to 10 μM S1P, whereas the levels of Ca^{2+} were not changed following 50 μM FBAL in HCT116 cells. (*H*) Levels of cAMP in cytoplasm following 10 μM S1P or 50 μM FBAL in HCT116 cells. (*I*) Levels of p-ERK and ERK in HCT116 cells following FBAL stimulation. pertussis toxin (PTX) (100 ng/mL) did not prevent the FBAL-induced higher expression of p-ERK. (*J*) Levels of p-ERK and ERK in HCT116 cells following S1P stimulation. PTX (100 ng/mL) significantly prevented the S1P-induced higher expression of p-ERK. (*K*) Western blotting analysis showing activation of RhoA in HCT116 cells. Data represent means ± SEM from three independent experiments performed in triplicate. **P* < 0.05, ***P* < 0.01, ****P* < 0.001, *****P* < 0.0001; ns: not significant, n = 3.

indicate that FBAL activates the ERK pathway through a β-arrestin1-dependent mechanism which is independent of Gαi, Gαq, and Gα12/13 signaling.

Ser343 in C-Terminus of S1PR2 Was the Key Site for the FBAL-Induced Phosphorylation of S1PR2. Since GRK6 mediates the phosphorylation of S1PR2 induced by FBAL, we further identified the phosphorylation site of S1PR2 using the following strategies: Co-IP coupled with mass spectrometry (Co-IP/MS) was performed to analyze the phosphorylation sites of S1PR2 (Fig. 6*A* and *SI Appendix,* Fig. S8*A*). MS analysis showed that, following FBAL, Thr342, Ser343, and Thr345 of the S1PR2 C-terminus might be the phosphorylation sites when treated with 50 μM FBAL (*SI Appendix,* Fig. S8 *B–D*). The C-terminus of S1PR2 was truncated and transfected into HEK293T cells. HEK293T$^{S1PR2\text{-}WT}$ cells did not exhibit a reduction in phosphorylated S1PR2 levels, whereas HEK293T$^{\Delta C}$ cells exhibited a remarkable reduction in phosphorylated S1PR2 level in response to FBAL treatment (Fig. 6*B*). Analysis of p-ERK, a downstream signaling event of phosphorylated S1PR2, indicated a time-dependent increase in HEK293T$^{S1PR2\text{-}WT}$ cells but not in HEK293T$^{\Delta C}$ cells (Fig. 6*C*). Using these methods, the C-terminus of S1PR2 was identified as the phosphorylation site for FBAL-induced phosphorylation of S1PR2.

The binding of β-arrestin to phosphorylated GPCR is crucial for modulating downstream signaling (32). Distinct phosphorylation modes affect the binding of GPCR to β-arrestins (37, 38). To clarify the effect of S1PR2 C-terminal truncation on its binding to β-arrestin1, we first generated S1PR2-knockout HCT116 cells by using CRISPR-Cas9, and then cotransfected them with the truncated S1PR2 construct and β-arrestin1. The Co-IP assay showed a strong binding of S1PR2 to β-arrestin1 in HCT116$^{KO\text{-}WT}$ cells, but not in HCT116$^{KO\text{-}\Delta C}$ cells following 50 μM FBAL (Fig. 6*D*). To identify which phosphorylation site (T342, S343, or T345) of S1PR2 was critical for the subsequent ERK pathway activation and β-arrestin1 recruitment, we generated a series of mutants by substituting T342, S343, and T345, individually or in combination, with alanine. As shown in Fig. 6*E*, the S343A single and triple mutations significantly prevented FBAL from activating the ERK pathway in HCT116$^{S1PR2\text{-}KO}$ cells. In contrast, ERK phosphorylation in response to FBAL was unaffected by T342A or T345A mutations. As shown in Fig. 6*F*, the S343A and triple alanine mutations abolished the ability of FBAL to promote the S1PR2–β-arrestin1 interaction. In contrast, mutation of T342A and T345A did not impair the FBAL-induced recruitment of β-arrestin1 to S1PR2. To mimic S1PR2 phosphorylation and its effect on downstream ERK pathway activation, we generated aspartic acid substitution mutants at residues T342, S343, and T345, both individually and in combination. As shown in Fig. 6*G*, both the S343D single and triple mutants promoted ERK pathway activation even without FBAL stimulation. Consistent with the above in vitro findings, HCT116$^{KO\text{-}S343A}$ cells orthotopically implanted in nude mice (Fig. 6 *H–J*) exhibited higher sensitivity than HCT116$^{KO\text{-}WT}$ cells to 5-FU. Taken together, Ser343 at the C-terminus of S1PR2 is the key site for FBAL-induced phosphorylation of S1PR2.

Activation of S1PR2 Engaged the β-arrestin-1-Dependent MEK/ERK/AP-1 Signaling Cascade, Leading to the Transcriptional Upregulation of *DPYD*. Activated S1PR2 signaling is transduced via the β-arrestin1/MEK/ERK pathway. Treatment with U0126 alone did not alter *DPYD* mRNA levels in HCT116 or SW620 cells (*SI Appendix,* Fig. S9*A*), indicating that basal MEK activity was not required to maintain baseline DPYD expression. However, when cells were exposed to the MEK inhibitor U0126 (39), FBAL failed to promote ERK phosphorylation or induce DPD expression in HCT116 and SW620 cells (Fig. 7*A* and *SI Appendix,* Fig. S9*B*), suggesting that FBAL-induced DPD upregulation depends on the MEK/ERK signaling pathway. To determine whether this regulation occurs at the transcriptional level, RT-qPCR analysis revealed that the MEK/ERK pathway modulates *DPYD* expression at the mRNA level in both HCT116 (Fig. 7*B*) and SW620 cells (*SI Appendix,* Fig. S9*C*).

MEK/ERK cascade signaling regulates a variety of transcription factors, such as ELK1, c-JUN, c-FOS, c-MYC, ATF1, and CREB. To identify the downstream signaling which transduces activated S1PR2, we analyzed p-c-JUN and p-c-FOS expression following stimulation with 50 μM FBAL. Western blotting of p-c-JUN and p-c-Fos showed a significant time-dependent increase in HCT116 cells (Fig. 7*C* and *SI Appendix,* Fig. S9*D*). As essential components of the AP-1 transcription factor complex, JUN and FOS can bind to specific cis-regulatory elements in promoters and induce target gene expression (40–42). Co-IP analysis revealed an interaction between c-JUN and c-FOS following FBAL (Fig. 7*D*). Ukon et al. reported that AP-1 participates in the regulation of *DPYD* transcription and that the AP-1 binding site −304/−279 on the promoter region is vital for activating *DPYD* transcription (43). To confirm the role of AP-1 in promoting *DPYD* transcription by binding to the promoter sequence of *DPYD*, we generated a luciferase reporter plasmid driven by a 2-kb fragment of the human *DPYD* promoter (upstream of the transcription start site) in HEK293T cells (Fig. 7 *E* and *F*). Upon exposure to FBAL (50 μM), an increase in *DPYD* luciferase reporter activity was detected (Fig. 7*G*). T-5224, a selective AP-1 inhibitor (44), blocked the binding of FOS/AP-1 to DNA without affecting its expression, and thereby attenuated FBAL-induced upregulation of DPD (Fig. 7 *H* and *I* and *SI Appendix,* Fig. S9 *E* and *F*). Taken together, FBAL promotes *DPYD* transcription via the MEK/ERK/AP-1 signaling pathway.

Discussion

In this study, we delineate a complete signaling axis through which the 5-FU catabolite FBAL actively drives chemoresistance. The study found that acting as a β-arrestin1-biased ligand of S1PR2, FBAL triggered a phosphorylation-dependent signaling cascade that culminated in the transcriptional upregulation of DPD, the rate-limiting enzyme for 5-FU inactivation. This study established a direct link between drug metabolism and receptor-mediated adaptive resistance.

The profound functional divergence between sustained versus transient activation of ERK signaling by FBAL and the endogenous ligand S1P, coupled with a complete lack of Gαi/q/12/13 engagement by FBAL originates from a fundamental difference in receptor phosphorylation. We identified GRK6, but not other GRKs, as the key kinase mediating this process, which is consistent with prior observations that GPCRs regulated by GRK5/6 are more prone to generating β-arrestin-biased signaling (45). The Ser343 residue located within the C-terminus of S1PR2 was identified as the key phosphorylation site responsible for influencing binding with β-arrestin1 (Figs. 5 and 6). This precise protein modification was necessary and sufficient to promote selective recruitment of β-arrestin1. This aligns with the "phosphorylation barcode" hypothesis, wherein overall ability of a phosphopeptide to bind β-arrestin1 also depends on the specific positions of phosphorylated residues rather than on their total number (37). Recent structural studies on GPCR–arrestin complexes such as GPR1 have revealed how distinct phosphorylation motifs and even cobound lipids can stabilize unique arrestin conformations, leading to diverse cellular outcomes such as internalization versus

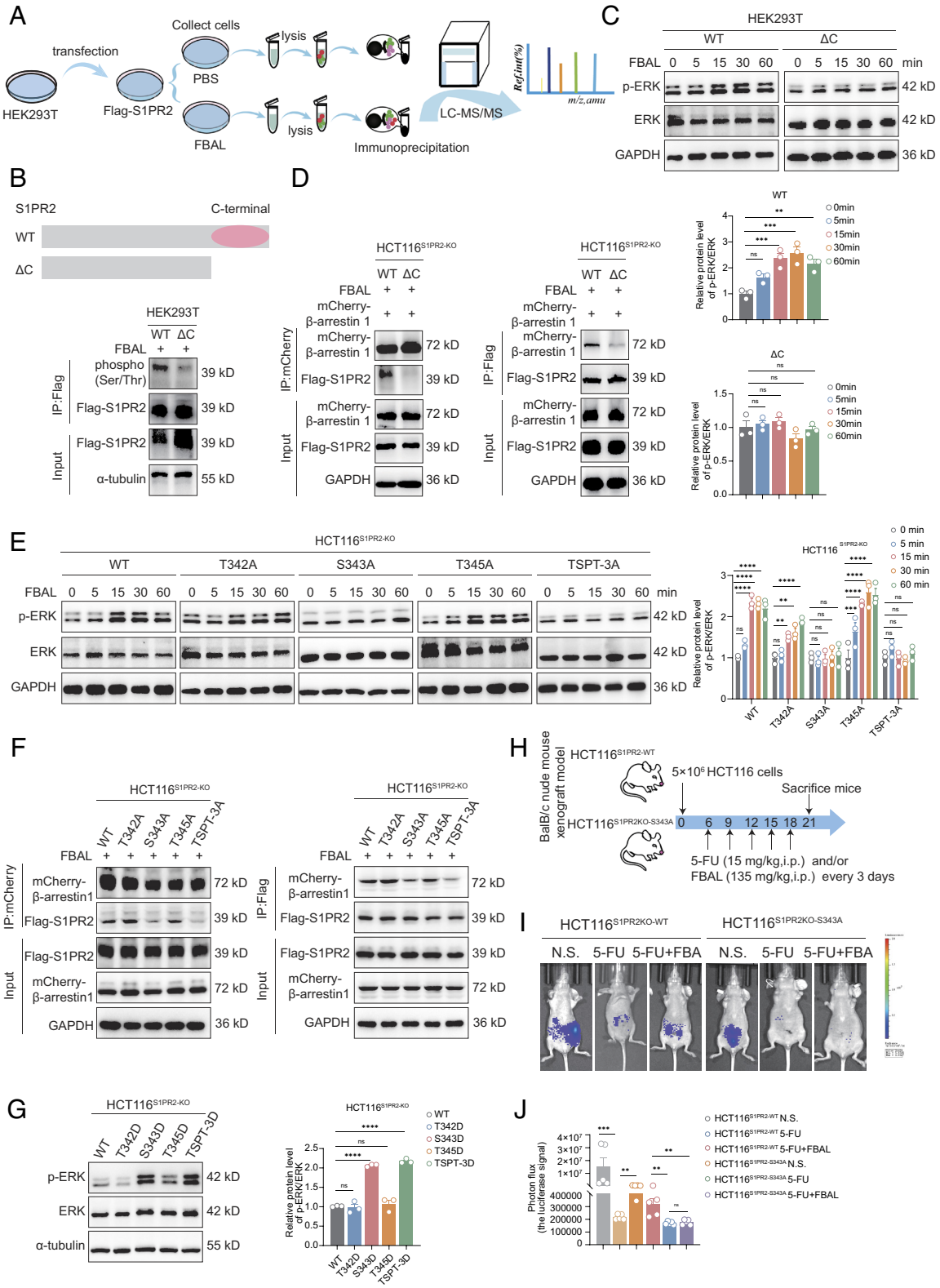

Fig. 6. Ser343 in C-terminus of S1PR2 was the key site for the FBAL-induced phosphorylation of S1PR2. (*A*) Schematic illustration of Co-IP combined with the LC-MS/MS assay for analyzing the phosphorylation sites of S1PR2. (*B*) Schematic representation of S1PR2 truncated mutants. Co-IP analysis of the phosphorylation level of S1PR2 in HEK293T cells transfected with full-length or truncated mutants of Flag-S1PR2. (*C*) Western blotting analysis of p-ERK and ERK in HEK293T cells transfected with full-length or truncated mutants of Flag-S1PR2 following 50 μM FBAL. (*D*) Co-IP analysis of the binding of S1PR2 with β-arrestin1 in HCT116^{S1PR2KO} cells cotransfected with the β-arrestin1-mCherry lentivirus and full-length or truncated mutants of Flag-S1PR2 following 50 μM FBAL stimulation. (*E*) Western blotting analysis of p-ERK and ERK in HCT116^{S1PR2KO} cells transfected with WT and alanine mutants of Flag-S1PR2 following 50 μM FBAL. (*F*) Co-IP analysis the binding of S1PR2 with β-arrestin1 in HCT116^{S1PR2KO} cells cotransfected with the S1PR2 mutants-Flag plasmids and the β-arrestin1-mCherry lentivirus. The binding of S1PR2 with the β-arrestin1 was observed following 50 μM FBAL. (*G*) Western blotting analysis of p-ERK and ERK in HCT116^{S1PR2KO} cells transfected with WT and aspartic acid mutants of Flag-S1PR2 without FBAL. (*H*) Schematic illustration of HCT116$^{S1PR2KO-WT}$ and HCT116$^{S1PR2KO-S343A}$ cells orthotopically implanted in nude mice. (*I*) HCT116$^{S1PR2KO-S343A}$ cells orthotopically implanted in nude mice, as compared to HCT116$^{S1PR2KO-WT}$ cells (*Left*), demonstrated greater sensitivity to 5-FU, with HCT116$^{S1PR2KO-S343A}$ xenografts almost disappearing despite coexposure to FBAL (*Right*). (*J*) Statistical analysis of total flux from IVIS bioluminescence images (n = 6). Data are mean ± SEM. **P* < 0.05, ***P* < 0.01, ****P* < 0.001, *****P* < 0.0001; ns: not significant, n = 3.

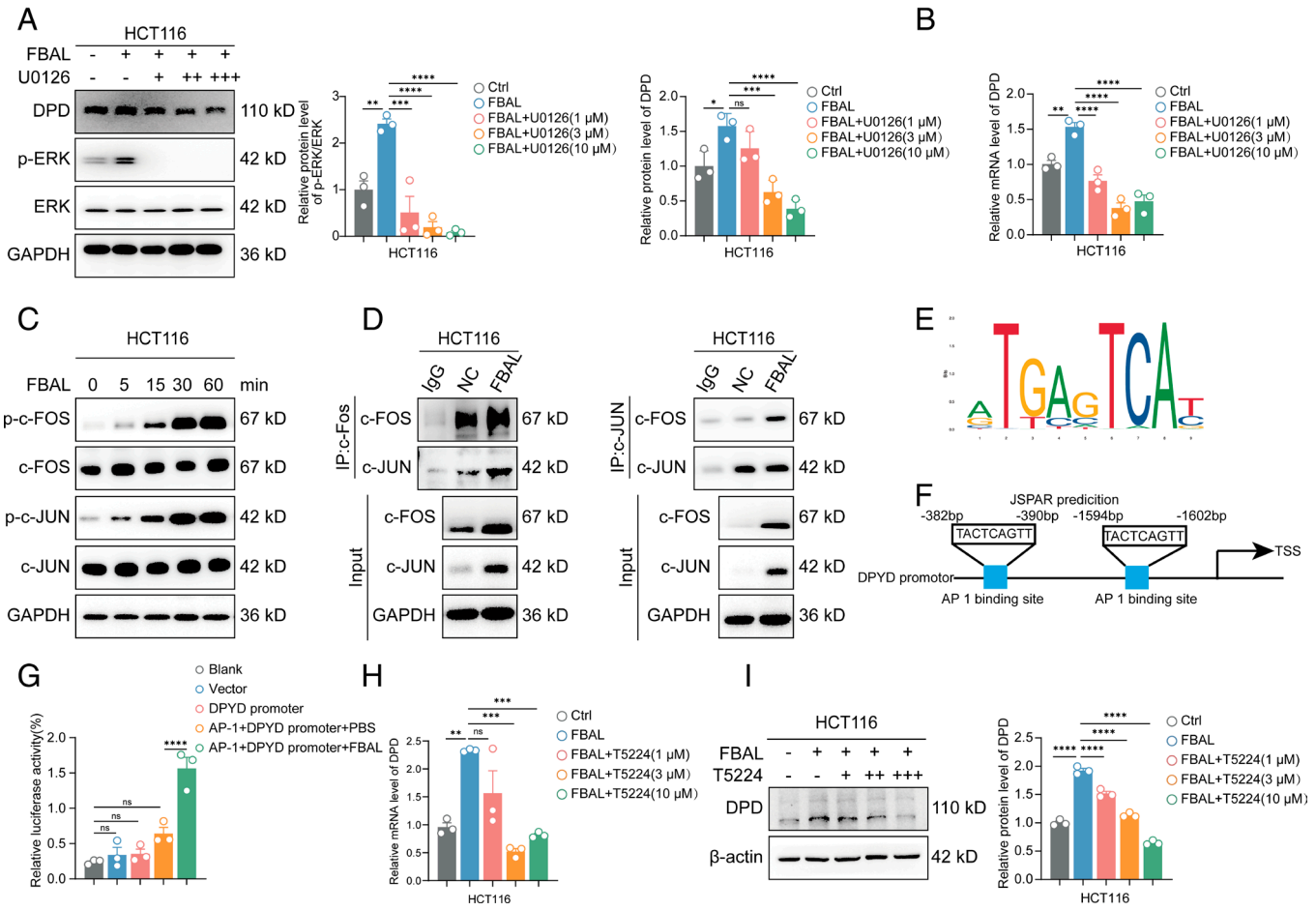

Fig. 7. Activation of S1PR2 engaged the β-arrestin-1-dependent MEK/ERK/AP-1 signaling cascade, leading to the transcriptional upregulation of *DPYD*. (*A*) Western blotting analysis of DPD, p-ERK, ERK, and GAPDH levels in HCT116 cells exposed to 50 μM FBAL and/or U0126. (*B*) RT-PCR assay showing *DPYD* mRNA levels in HCT116 cells exposed to 50 μM FBAL and/or U0126. (*C*) Western blotting analysis of p-c-JUN, c-JUN, p-c-FOS, c-FOS, and GAPDH levels in HCT116 cells exposed to 50 μM FBAL. (*D*) Co-IP assay showed the binding of c-JUN with c-FOS in HCT116 cells following 50 μM FBAL. (*E*) AP-1 response element motif sequences. (*F*) Bioinformatic analysis of the potential AP-1 binding sites in the 2 kb *DPYD* promoter region using the Jaspar database. (*G*) Luciferase assay of *DPYD* promoter. Cotransfection of HEK293T cells with AP-1 and *DPYD* promoter pGL3-Luciferase constructs, followed by treatment with 50 μM FBAL. (*H*) *DPYD* mRNA levels in HCT116 cells exposed to 50 μM FBAL and/or T-5224. (*I*) Western blotting analysis of DPD and β-actin levels in HCT116 cells exposed to 50 μM FBAL and/or T-5224. Data are mean ± SEM. **P* < 0.05, ***P* < 0.01, ****P* < 0.001, *****P* < 0.0001; ns: not significant, n = 3.

sustained signaling (46). By analogy, we proposed that GRK6-mediated phosphorylated-Ser343 (pSer343) constitutes the core element of the S1PR2 barcode. This barcode is preferentially decoded by β-arrestin1 to form a stable signaling complex that drives sustained ERK/AP-1 activity, rather than a transient or desensitizing signal. Thus, our work provides a concrete molecular example of how a single metabolite, through a specific kinase and phosphorylation site, can reprogram the signaling destiny of a receptor by rewriting its intracellular barcode.

Notably, we observed distinct kinetic patterns of DPD expression induced by S1PR2 agonists S1P and FBAL, with S1P triggering a rapid increase in DPD expression as early as 5 min, while FBAL-mediated DPD upregulation persisted for up to 60 min- a temporal discrepancy that raises consideration of potential non-transcriptional regulatory mechanisms. However, multiple lines of evidence support that the rapid 5-min induction of DPD by S1PR2 activation is predominantly driven by transcriptional regulation, rather than posttranscriptional pathways. Classically, rapid transcriptional activation within several minutes of extracellular stimulation has been well documented; landmark research confirmed that membrane-originated signaling can promptly activate preassembled nuclear transcriptional machinery, enabling robust gene transcription initiation within 5 min upon growth factor stimulation (47). Mechanistically, this rapid transcription is underpinned by poised RNA polymerase II and preexisting DNA-bound transcription factor complexes, which can be instantly modulated by GPCR and Rho GTPase signaling without de novo protein synthesis (48), providing a direct mechanistic paradigm for our observed fast DPD induction. In contrast, FBAL acts as a β-arrestin biased S1PR2 agonist, triggering sustained β-arrestin/ERK signaling that accounts for the prolonged DPD elevation up to 60min. Such kinetic differences therefore reinforce, rather than contradict, the transcriptional regulatory model of DPD expression. We also acknowledge that posttranscriptional or protein stabilization mechanisms could contribute to the early phase of DPD induction. Future studies using transcriptional inhibitors (e.g., actinomycin D) or translational inhibitors (e.g., cycloheximide) will help definitively parse transcriptional versus posttranscriptional contributions. Nevertheless, given that our promoter activity assays clearly demonstrate S1PR2-dependent transcriptional activation, and given the extensive precedent for rapid transcriptional induction in the literature, we favor transcription as the dominant mechanism underlying DPD upregulation.

Traditionally viewed as an inactive toxin responsible for off-target tissue damage, FBAL has been redefined herein as an active driver of on-target therapy failure. This dual role of mediating both systemic toxicity and tumor-specific resistance has direct clinical implications, and suggests that patients experiencing severe FBAL-related toxicity

may have tumors concurrently exposed to higher FBAL concentrations (49), potentially exacerbating their resistance. Conversely, monitoring FBAL levels could inform both toxicity risk and resistance propensity. Our study suggests a unified therapeutic strategy targeting the FBAL/S1PR2 axis. We found that using S1PR2 antagonist, JTE-013, or silencing S1PR2 can restore 5-FU sensitivity (Figs. 1 and 2), thus validating this hypothesis. Although we did not include a JTE-013-alone control in the initial in vivo experiment, our subsequent genetic loss-of-function studies (S1PR2 knockdown) provide unequivocal evidence that the resistance-reversing effect is specifically mediated by S1PR2 inhibition, not by off-target antitumor activity of JTE-013 (Fig. 2 *E–G*). Collectively, these findings establish the FBAL/S1PR2 axis as a viable therapeutic target and demonstrate that pharmacological or genetic disruption of this pathway effectively re-sensitizes tumors to 5-FU, offering a rationale for combining S1PR2 antagonists with fluoropyrimidine-based chemotherapy to overcome acquired resistance. More selectively, disrupting the phosphorylation-dependent interface between pSer343-S1PR2 and β-arrestin1 could inhibit the resistance pathway while potentially sparing other S1PR2 functions. This approach exemplifies the therapeutic potential of inhibiting specific pathology-driven biased signaling pathways.

Our findings extend beyond 5-FU resistance and offer a framework for understanding how tumors may exploit GPCRs to adapt to therapeutic stress. First, we highlighted the drug metabolites themselves are a source of biologically active GPCR ligands within the therapy-altered tumor microenvironment. This paradigm prompts a reevaluation of other nucleoside analogs or metabolic therapies whose catabolites may similarly act as "stealth" agonists. Second, our work underscores how β-arrestin-biased signaling acts as a potent mediator of pro-survival adaptation. Although often associated with receptor desensitization, β-arrestins are increasingly being recognized for their ability to scaffold sustained kinase signals. Therefore, resistance mechanisms characterized by persistent ERK or AKT activation should be scrutinized for upstream GPCR and β-arrestin involvement. Finally, the critical role of GRK6 reveals kinase specificity as a key control point. Given that GRK expression is frequently altered in cancers (50), the cellular kinome may predispose tumors to specific ligand-induced biased signaling, suggesting that GRK isoforms are predictive biomarkers or therapeutic targets.

In summary, we have identified a coherent molecular circuit linking 5-FU metabolism to acquired resistance. FBAL acts as a biased agonist for S1PR2, engaging a GRK6/β-arrestin1/ERK/AP-1 pathway to upregulate DPD expression. This study redefined FBAL from a toxic byproduct to a central driver of resistance and established a specific phosphorylation-dependent interface of S1PR2 as a promising target for restoring chemosensitivity in 5-FU-resistant cancers.

Materials and Methods

Reagents. Primary antibodies used for western blotting, IP, Immunohistochemistry (IHC), and immunofluorescence (IF) are listed in *SI Appendix,* Table S1. The siRNAs and shRNAs corresponding to the target sequences were synthesized by GenePharma Technology (Suzhou, China), and the corresponding sequences are listed in *SI Appendix,* Table S2. The primer sequences used in the qPCR experiments are listed in *SI Appendix,* Table S3. The plasmids used in the study were synthesized by GenePharma Technology (Suzhou, China), and the corresponding sequences are listed in *SI Appendix,* Table S4. All chemicals used in this study are listed in *SI Appendix,* Table S5. Detailed descriptions of the other materials and reagents are provided in the Supporting Information and in *SI Appendix,* Tables S1–S8. All detailed methods are provided in *SI Appendix*. Details of the mouse studies, including the subcutaneous xenograft model and colorectal cancer orthotopic model, are presented in *SI Appendix*.

Statistical Analysis. Graphical representations and statistical analyses were performed using GraphPad Prism 8. The number of biological replicates in each experiment is indicated in the Figure legend. Data are presented as means ± SEM. Differences between means were determined using unpaired Student's *t* test or one-way ANOVA. Differences were considered significant at $P < 0.05$.

Ethical Approval. The Animal Welfare Committee of Capital Medical University approved the experimental protocols for the animal studies (AEEI-2023-214).

Data, Materials, and Software Availability. All study data are included in the article and/or supporting information.

ACKNOWLEDGMENTS. We gratefully acknowledge the support from the Joint Laboratory for Research and Treatment of Spinal Cord Injury in Spinal Deformity, Laboratory for Clinical Medicine, as well as the invaluable assistance of Professor Hu Jia from the Core Facilities Center, all at Capital Medical University, Beijing, China. This study was supported by the National Natural Science Foundation of China (Grant No. 82173841).

1. A. T. Pirzaman *et al.*, 5-flourouracil-induced toxicity in both male and female reproductive systems: A narrative review. *Hum. Exp. Toxicol.* **42**, 9603271231217988 (2023).
2. S. Chatterjee *et al.*, Ribosome quality control mitigates the cytotoxicity of ribosome collisions induced by 5-fluorouracil. *Nucleic Acids Res.* **52**, 12534–12548 (2024).
3. W. H. Gmeiner, C. C. Okechukwu, Review of 5-FU resistance mechanisms in colorectal cancer: Clinical significance of attenuated on-target effects. *Cancer Drug Resist.* **6**, 257–272 (2023).
4. L. M. Henricks *et al.*, DPYD genotype-guided dose individualisation of fluoropyrimidine therapy in patients with cancer: A prospective safety analysis. *Lancet Oncol.* **19**, 1459–1467 (2018).
5. T. J. Wigle, E. V. Tsvetkova, S. A. Welch, R. B. Kim, DPYD and fluorouracil-based chemotherapy: Mini review and case report. *Pharmaceutics* **11**, 199 (2019).
6. R. Wu *et al.*, Histone h3k27 trimethylation modulates 5-fluorouracil resistance by inhibiting PU.1 binding to the DPYD promoter. *Cancer Res.* **76**, 6362–6373 (2016).
7. C. Franck, P. Malfertheiner, M. Venerito, Safe administration of s-1 after 5-fluorouracil-induced cardiotoxicity in a patient with colorectal cancer. *BMJ Case Rep.* **2017**, bcr2016219162 (2017).
8. A. Reis-Mendes *et al.*, The main metabolites of fluorouracil + adriamycin + cyclophosphamide (FAC) are not major contributors to FAC toxicity in h9c2 cardiac differentiated cells. *Biomolecules* **9**, 98 (2019).
9. Z. Guo *et al.*, Activation of sphingosine-1-phosphate receptor 2 (S1PR2) upregulates dihydropyrimidine dehydrogenase (DPD) expression in colon cancer cells. *J. Adv. Res.* **77**, 497–511 (2025).
10. Y. Duan *et al.*, A detrimental role of endothelial s1PR2 in cardiac ischemia-reperfusion injury via modulating mitochondrial dysfunction, NLRP3 inflammasome activation, and pyroptosis. *Redox Biol.* **75**, 103244 (2024).
11. Y. Wang *et al.*, The role of sphingosine 1-phosphate receptor 2 in bile-acid-induced cholangiocyte proliferation and cholestasis-induced liver injury in mice. *Hepatology.* **65**, 2005–2018 (2017).
12. S. Mu *et al.*, Inhibition of sphingosine-1-phosphate receptor-2 attenuates idiopathic pulmonary fibrosis by preventing its binding to dapper1 in bronchial epithelial cells. *Br. J. Pharmacol.* **183**, 957–972 (2026).
13. D. Luo *et al.*, Rational design, synthesis, and biological evaluation of novel S1PR2 antagonists for reversing 5-FU-resistance in colorectal cancer. *J. Med. Chem.* **65**, 14553–14577 (2022).
14. Z. Zhang *et al.*, Distinct phosphorylation patterns of AT1R by biased ligands and GRK subtypes. *Int. J. Mol. Sci.* **26**, 7988 (2025).
15. J. Yang, X. Tang, Z. Liang, M. Chen, L. Sun, Taurocholic acid promotes hepatic stellate cell activation via s1PR2/p38 MAPK/YAP signaling under cholestatic conditions. *Clin. Mol. Hepatol.* **29**, 465–481 (2023).
16. N. Very *et al.*, Thymidylate synthase o-GlcNAcylation: A molecular mechanism of 5-FU sensitization in colorectal cancer. *Oncogene* **41**, 745–756 (2022).
17. Y. H. Zhang, D. D. Luo, S. B. Wan, X. J. Qu, S1PR2 inhibitors potently reverse 5-FU resistance by downregulating DPD expression in colorectal cancer. *Pharmacol. Res.* **155**, 104717 (2020).
18. L. Li *et al.*, The upregulation of dihydropyrimidine dehydrogenase in liver is involved in acquired resistance to 5-fluorouracil. *Eur. J. Cancer* **49**, 1752–1760 (2013).
19. R. Wu *et al.*, S1PR-targeted PET imaging: Advancing insights into neuroinflammatory and immune-related pathologies. *Mol. Pharm.* **23**, 66–78 (2026).
20. J. S. Smith *et al.*, Noncanonical scaffolding of g(alphai) and beta-arrestin by g protein-coupled receptors. *Science* **371**, eaay1833 (2021).
21. R. Chen, X. Cai, J. Liu, B. Bai, X. Li, Sphingosine 1-phosphate promotes mesenchymal stem cell-mediated cardioprotection against myocardial infarction via ERK1/2-MMP-9 and Akt signaling axis. *Life Sci.* **215**, 31–42 (2018).
22. T. Chen *et al.*, Sphingosine-1 phosphate promotes intestinal epithelial cell proliferation via s1PR2. *Front. Biosci.* **22**, 596–608 (2017).
23. R. Liu *et al.*, Conjugated bile acids promote cholangiocarcinoma cell invasive growth through activation of sphingosine 1-phosphate receptor 2. *Hepatology.* **60**, 908–918 (2014).
24. S. K. Shenoy *et al.*, Beta-arrestin-dependent, g protein-independent ERK1/2 activation by the beta2 adrenergic receptor. *J. Biol. Chem.* **281**, 1261–1273 (2006).
25. A. N. Ives *et al.*, Middle-down mass spectrometry reveals activity-modifying phosphorylation barcode in a class C G protein-coupled receptor. *J. Am. Chem. Soc.* **144**, 23104–23114 (2022).
26. A. Patwardhan, N. Cheng, J. Trejo, Post-translational modifications of G protein-coupled receptors control cellular signaling dynamics in space and time. *Pharmacol. Rev.* **73**, 120–151 (2021).
27. Q. Chen *et al.*, Structures of rhodopsin in complex with g-protein-coupled receptor kinase 1. *Nature* **595**, 600–605 (2021).

28. J. Duan *et al.*, GPCR activation and GRK2 assembly by a biased intracellular agonist. *Nature* **620**, 676–681 (2023).
29. E. Reiter, R. J. Lefkowitz, GRKs and beta-arrestins: Roles in receptor silencing, trafficking and signaling. *Trends Endocrinol. Metab.* **17**, 159–165 (2006).
30. D. E. Uehling *et al.*, Design, synthesis, and characterization of 4-aminoquinazolines as potent inhibitors of the G protein-coupled receptor kinase 6 (GRK6) for the treatment of multiple myeloma. *J. Med. Chem.* **64**, 11129–11147 (2021).
31. H. V. Waldschmidt *et al.*, Structure-based design of highly selective and potent G protein-coupled receptor kinase 2 inhibitors based on paroxetine. *J. Med. Chem.* **60**, 3052–3069 (2017).
32. J. Janetzko *et al.*, Membrane phosphoinositides regulate GPCR-beta-arrestin complex assembly and dynamics. *Cell* **185**, 4560–4573 (2022).
33. R. Ranjan, H. Dwivedi, M. Baidya, M. Kumar, A. K. Shukla, Novel structural insights into GPCR-beta-arrestin interaction and signaling. *Trends Cell Biol.* **27**, 851–862 (2017).
34. A. Inoue *et al.*, Illuminating g-protein-coupling selectivity of GPCRs. *Cell* **177**, 1933–1947 (2019).
35. R. T. Windh *et al.*, Differential coupling of the sphingosine 1-phosphate receptors edg-1, edg-3, and h218/edg-5 to the g(i), g(q), and g(12) families of heterotrimeric g proteins. *J. Biol. Chem.* **274**, 27351–27358 (1999).
36. Z. Tang *et al.*, Pertussis toxin reduces calcium influx to protect ischemic stroke in a middle cerebral artery occlusion model. *J. Neurochem.* **135**, 998–1006 (2015).
37. N. R. Latorraca *et al.*, How GPCR phosphorylation patterns orchestrate arrestin-mediated signaling. *Cell* **183**, 1813–1825 (2020).
38. X. E. Zhou *et al.*, Identification of phosphorylation codes for arrestin recruitment by g protein-coupled receptors. *Cell* **170**, 457–469 (2017).
39. T. Wang *et al.*, The MEK inhibitor u0126 ameliorates diabetic cardiomyopathy by restricting XBP1's phosphorylation dependent SUMOylation. *Int. J. Biol. Sci.* **17**, 2984–2999 (2021).
40. P. Angel, M. Karin, The role of jun, fos and the AP-1 complex in cell-proliferation and transformation. *Biochim. Biophys. Acta* **1072**, 129–157 (1991).
41. E. O. Karakaslar *et al.*, Transcriptional activation of jun and fos members of the AP-1 complex is a conserved signature of immune aging that contributes to inflammaging. *Aging Cell* **22**, e13792 (2023).
42. D. Song, Y. Lian, L. Zhang, The potential of activator protein 1 (AP-1) in cancer targeted therapy. *Front. Immunol.* **14**, 1224892 (2023).
43. K. Ukon *et al.*, Activator protein accelerates dihydropyrimidine dehydrogenase gene transcription in cancer cells. *Cancer Res.* **65**, 1055–1062 (2005).
44. H. S. Shim *et al.*, TERT activation targets DNA methylation and multiple aging hallmarks. *Cell* **187**, 4030–4042 (2024).
45. E. S. F. Matthees *et al.*, GRK specificity and gβγ dependency determines the potential of a GPCR for arrestin-biased agonism. *Commun. Biol.* **7**, 802 (2024).
46. H. Cai *et al.*, Noncanonical agonist-dependent and -independent arrestin recruitment of GPR1. *Science* **390**, eadt8794 (2025).
47. M. E. Greenberg, E. B. Ziff, Stimulation of 3t3 cells induces transcription of the c-fos proto-oncogene. *Nature* **311**, 433–438 (1984).
48. C. S. Hill, J. Wynne, R. Treisman, The rho family GTPases RhoA, rac1, and CDC42hs regulate transcriptional activation by SRF. *Cell* **81**, 1159–1170 (1995).
49. Y. Yamada *et al.*, Plasma concentrations of 5-fluorouracil and f-beta-alanine following oral administration of s-1, a dihydropyrimidine dehydrogenase inhibitory fluoropyrimidine, as compared with protracted venous infusion of 5-fluorouracil. *Br. J. Cancer* **89**, 816–820 (2003).
50. L. Nogués *et al.*, G protein-coupled receptor kinases (GRKs) in tumorigenesis and cancer progression: Gpcr regulators and signaling hubs. *Semin. Cancer Biol.* **48**, 78–90 (2018).